Markus Andres*, Karim Ishak, Wolfgang Menzel and Hans-Ludwig Bloecher

# Extraction of Micro-Doppler Signatures using Automotive Radar Sensors

**Abstract:** Detection of pedestrians in an urban environment is a highly sophisticated task. This paper presents a signal processing technique suitable for frequency-modulated continuous wave (FMCW) radar sensors using chirp sequence modulation, allowing observation of slow-moving objects with high resolution capability in range and velocity. Velocity resolution can be improved through auto-regressive linear prediction (AR-LP) without requiring a long chirp sequence duration. Furthermore, the influence of the frequency deviation used and velocity resolution will be shown in a scenario with two objects. An adaptive velocity resolution improvement will be presented to extract a characteristic micro-Doppler signature (μD-signature) of a slowly moving pedestrian, a car, and an inline-skater. This is verified by measurements at the carrier frequency of 77 GHz.

**Keywords:** chirp sequence modulation, pedestrian detection, linear prediction, 76–81 GHz, micro-Doppler

**PACS® (2010).** 84

***Corresponding author: Markus Andres:** Institut of Microwave Techniques, University Ulm, 89081 Ulm, Germany
E-mail: markus.andres@uni-ulm.de
**Karim Ishak:** Institut of Microwave Techniques, University Ulm, 89081 Ulm, Germany
**Wolfgang Menzel:** Institut of Microwave Techniques, University Ulm, 89081 Ulm, Germany
**Hans-Ludwig Bloecher:** Group Research and Advanced Engineering, Daimler AG, 89013 Ulm, Germany

## 1 Introduction

Nowadays, automotive radar sensors are widely used for driver assistance systems to realize comfort and safety functions. Due to the increased traffic density in megacities, the demand for pedestrian protection is increasing. Extended environmental information is required to assure stable and reliable safety functions. Radar sensors are essential for delivering robust target information, effectively monitoring pedestrians in critical situations and avoiding or mitigating accidents. To monitor slowly moving pedestrians, good separation abilities in angle, range, and velocity have to be ensured for radar sensors. By shifting the operating frequency from 24 GHz to 77 GHz or 79 GHz the Doppler frequency of a moving object increases approximately threefold due to the shorter wavelength improving the detection of slow movements of a pedestrian through an increased Doppler-shift.

However, the field study [1] shows that the traveling speed of pedestrians varies depending on the situation, weather condition, and age of the observed person. As an example, the mean pedestrian speed for 7123 differently-aged pedestrians while crossing a street with traffic lights under different weather conditions is 1.25–1.51 m/s (4.5–5.4 km/h) [1]. If a pedestrian walks closely by a standing car, the separation ability in range or angle of the radar sensor might not be adequate enough. Hence, the separation needs to be done in velocity.

Reference [2] has shown that a pulse-Doppler radar can be used to extract additional velocity information of the movement of a person by Short Time Fourier Transform (STFT). A high velocity resolution capability within one range-angular cell is sufficient to determine a specific micro-Doppler signature of one object. However, good velocity resolution is dependent on the measurement time of the sensor, a contradiction to the required short reaction time in typical traffic situations. Of course, the observation time of slowly moving targets is also influenced by the field of view and squint angle of the radar sensor, as well as the relative velocity and distance between sensor and target.

In the following a signal processing algorithm will be presented increasing the velocity resolution without changing the measurement time and without using STFT to extract micro-Doppler (μD).

## 2 Range-Doppler processing

Frequency modulated continuous wave (FMCW) radars are commonly used for automotive applications. On the radar sensor market, several modulation techniques based on FMCW processing exist. Different tier-one suppliers for original equipment manufacturers (OEM) of radar sensor systems are currently using the chirp sequence modulation rather than triangular FMCW modulation. The latter technique offers the advantages of independent range and velocity processing, easy target suppression in certain velocity areas, reduced ambiguity for velocity processing, variable adjustment of the maximum velocity within the velocity span, and separate Fast Fourier Transformations (FFT) for range and velocity processing.

However, FMCW radar sensors are limited by the fixed frequency deviation and the chirp sequence duration of the transmitted signal, affecting the range and velocity resolution. By using advanced signal processing techniques as presented in this paper, the resolution capability for velocity can be improved without changing the hardware setup and can be adapted to the observed scene.

## 2.1 Chirp sequence modulation

Chirp sequence modulation, also known as fast chirp modulation, is based primarily on the transmission of saw tooth FMCW signals at the transmit frequency $f_{\mathrm{TX}}$ and with a steep slope $S$ as depicted in Fig. 1. Each frequency ramp (chirp) sweeps with a frequency deviation $B$ within a very short chirp time $T$, e.g. 20–200 µs, around the center frequency $f_c$. According to the steep slope, the intermediate frequency resulting from the time of flight of a reflected signal is typically much larger than a usual Doppler frequency shift.

The radar sensor transmits $K$ successive chirps with a constant ramp repetition interval $T_{\mathrm{RRI}}$ in the measurement time $T_{\mathrm{meas}}$. The back-scattered and down-converted time domain signal of all chirps $s_{\mathrm{IF}}(t)$ for a single and constant moving target with a radial velocity $v_r$ in the distance $R$ results in [3]:

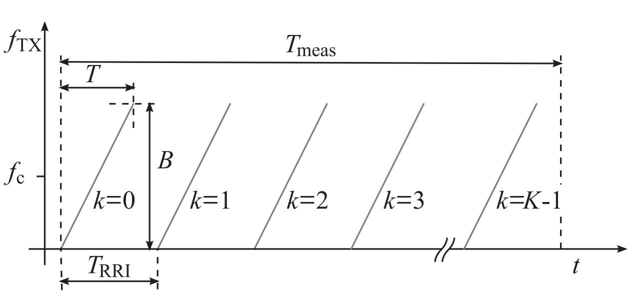


**Fig. 1:** Chirp sequence modulation scheme with $K$ successive chirps.

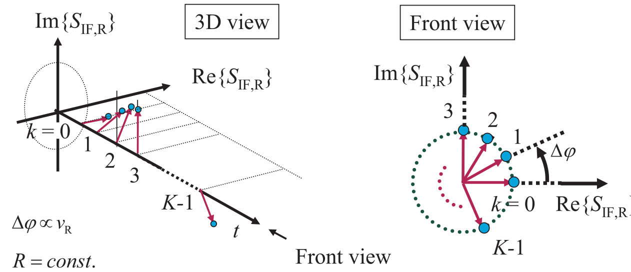


**Fig. 2:** Scheme of the phase-shifted complex range samples $k$ of one chirp sequence, containing a moving target at one fixed range cell [4].

$$s_{\mathrm{IF}}(t) = e^{j 2\pi (2 f_c \cdot R / c_0)} \cdot \sum_{k=0}^{K-1} e^{j 2\pi \cdot \left[ \frac{2 f_c \cdot v_r \cdot T_{\mathrm{RRI}} \cdot k}{c_0} + \left( \frac{2 f_c \cdot v_r}{c_0} + \frac{2 B \cdot R}{T \cdot c_0} \right) t \right]} \cdot \mathrm{rect}\left( \frac{t - k \cdot T_{\mathrm{RRI}}}{T} \right). \quad (1)$$

In a first step, an FFT is performed for $N$ sampling points of each chirp $k$, resulting in $N/2$ range cells. Assuming that a target is moving with a constant radial velocity $v_r$ in one range cell, the precise range of the target differs slightly and causes a constant phase difference $\Delta\varphi$ between two successive chirps. Hence, target velocity and constant phase difference are directly proportional. Fig. 2 shows the rotation of the complex range vector over time with constantly increasing phase, affected by the target movement. Moreover, the signum and hence the rotation direction of all complex range samples depend on the moving direction of the target. Applying the Fourier Transform to the complex range vector over the $K$ chirps results in one discrete frequency peak, if only one target is present. This frequency corresponds to the relative velocity of the target. In total, $N/2 \cdot K$ FFTs are required.

The maximum unambiguous range $R_{\max}$ of the processing

$$R_{\max} = \frac{c_0 T}{2B} \cdot \frac{f_s}{2} \quad (2)$$

is mainly limited by the sampling interval $T_s$ (sampling frequency $f_s = 1/T_s$) of the time domain signal of the baseband, considering a constant slope $S = B/T$ and a sufficient SNR of the target. Furthermore, the maximum velocity $v_{r,\max,1}$

$$\left| v_{r,\max,1} \right| = \frac{c_0}{2 T_{\mathrm{RRI}}} \cdot \frac{1}{2 f_c} \quad (3)$$

is limited by the ramp repetition interval to fulfill the sampling theorem in the Doppler-domain. As a prerequisite, the target has to be within one range cell to avoid range cell migration. Thus, the maximum velocity $v_{r,max,2}$ has also to be less than

$$\left|v_{r,max,2}\right| = \frac{c_0}{2T_{RRI}} \cdot \frac{1}{B \cdot K} \quad (4)$$

to avoid range-Doppler coupling of the neighboring range/velocity bins [5] leading to a degradation of the velocity resolution.

As an example, using a carrier frequency of around 77 GHz, a frequency deviation of 1.5 GHz, $T_{RRI} = 160$ µs, and $K = 96$, the maximum radial velocity equals to $v_{r,max,1} =$ 21.9 km/h and $v_{r,max,2} = 23.42$ km/h. Leading to the maximum tolerable absolute velocity of 21.9 km/h $\left(\left|v_{r,max,1}\right| < \left|v_{r,max,2}\right|\right)$.

## 2.2 Improvement of Doppler resolution

The velocity resolution $\Delta v$ in chirp sequence modulation is given as:

$$\Delta v = \frac{c_0}{2 f_c \cdot T_{RRI} \cdot K} \quad (5)$$

and can be improved by increasing the amount of chirps $K$ as considering a constant $T_{RRI}$. Consequently, the measurement time $T_{meas}$ will be increased.

The conflict between short measurement time and high velocity resolution can be tackled by signal post-processing. Spectral signal estimation methods, like the auto-regressive linear prediction (AR-LP), which will be applied in the following, show a robust performance if sufficient signal-to-noise ratio (SNR) is available. The aim of this algorithm is to establish an appropriate auto-regressive filter model depending on the original input signal [6], [7]. The coefficients of this filter model are determined with Burg's-Method by minimizing the error between model and sampled signal. This model than allows prediction of successive samples in the forward and/or backward direction to extend the original number of measurement values.

Fig. 3 shows the scheme of the artificial increase of the $K$ measured complex range samples by forward AR-LP. It is assumed that a single target is moving with a constant velocity. The prediction of the samples results in the harmonic extension of the original signal. The calculation of the Fourier Transformation of this extended signal improves the velocity resolution and narrows the Doppler frequency peak without increasing the measurement time. In this way, the required velocity resolution can be adapted to the observed scene focusing on the region of interest. Of course, AR-LP also has some limitations. The order of the underlying AR filter model has to be fixed to the maximum number of physical targets and their Doppler contributions within one range cell. Measurements have shown that using 16 to 31 filter coefficients lead to an improvement of the velocity resolution by a factor of 2 to 4.

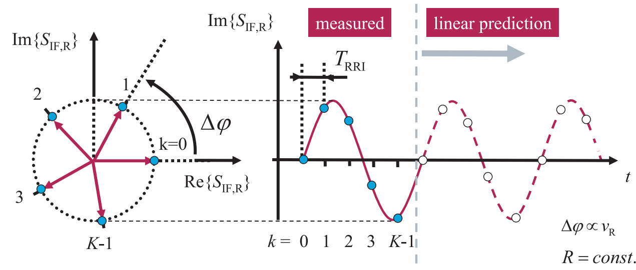


**Fig. 3:** Scheme of the extension of the complex range samples by AR-LP processing of one target at a fixed range cell, and constant velocity [4].

# 3 Observation of a moving pedestrian

## 3.1 Chirp sequence processing model

A radar signal processing model for automotive radar sensors was designed on the basis of the chirp sequence modulation.

The received and down-converted time domain signals of all chirps received by the radar sensor are sampled, AD-converted and stored on the hard drive of a PC. Then the data are fed to the input of the range processor. After windowing and Fourier transforming the time domain signal of each chirp, the velocity processing is applied. To improve the velocity resolution, each same range cells of successive chirps can again be extended by AR-LP. Applying windowing again reduces the leakage effect for FFT processing. A range-velocity matrix is provided at the output of the signal processing model.

## 3.2 Sensor setup

In the following, the chirp sequence processing model was applied to the received signals of a monostatic radar sensor [8] with a vertical polarized lens horn antenna with

| Parameter | Setup 1 | Setup 2 using AR-LP |
|---|---|---|
| Start frequency | 77 GHz | 77 GHz |
| Frequency deviation | 1.5 GHz | 1.5 GHz |
| Polarisation | vertical | vertical |
| Amount of Chirps | 32 | 32 + 64 artificial |
| Ramp rep. intervall | 160 μs | 160 μs |
| Measurement time | 5.1 ms | 5.1 ms |
| Velocity Resolution | 1.36 km/h | 0.45 km/h |
| Max. Range | 49.9 m | 49.9 m |
| Max. velocity | ±21.9 km/h | ±21.9 km/h |

**Table I:** Technical Data Of the Radar System Using Chirp Sequence Modulation

a one-way half-power beam width of 4.1° in azimuth and 3.1° in elevation. Table I shows the radar sensor parameters. The radar sensor was operating with a starting frequency of 77 GHz and a frequency deviation of 1.5 GHz. Due to the long $T_{RRI}$ of 160 μs, the unambiguous velocity span is limited to ±21.9 km/h. The effective frequency deviation of the following results are adjusted after data acquisition by taking into account only the respective part of data of each chirp.

### 3.3 Measurement results

In the following, the separation of a pedestrian passing a standing car is investigated with different range and velocity resolutions. The car was located at a distance of 10 m without lateral displacement to the sensor, and the pedestrian was passing the car at a walking speed of 4.5 km/h and a spacing of 60 cm to the left car body shell.

The measurement results are depicted in Fig. 4. The main scattering centers of the car are located at 10.4 m, 11.5 m, and 12.2 m and show a velocity of 0 km/h. The pedestrian instead exhibits a scattering center at 10.5 m with a radial velocity of 4.5 km/h. Fig. 4 (a) shows that, when using an effective frequency deviation of 0.5 GHz, the scattering centers of the car and the pedestrian merge at the distance of 10.5 m due to superposition of the back-scattered waves of the car body shell and the pedestrian. Such a superposition can influence the separation capability and can lead to a loss of detection of two neighboring targets. This effect can be reduced by separating the scattering centers of an object either in velocity or range. Fig. 4 (b) depicts the measurement result after improving the velocity resolution from 1.36 km/h to 0.45 km/h by AR-LP (32 real chirps + 64 artificial chirps) for an effective frequency deviation of 0.5 GHz. It can be seen that the two peaks of the pedestrian and the car can be separated. Increasing the effective frequency deviation

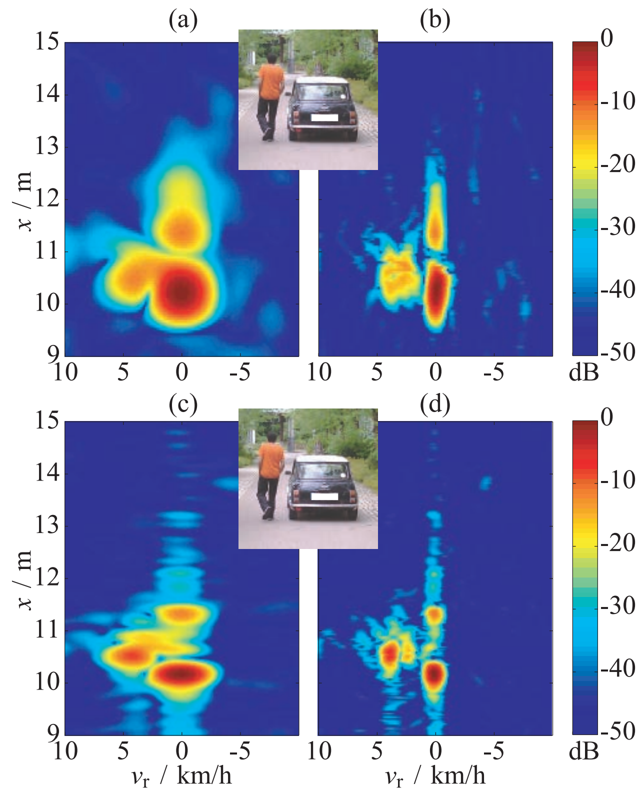


**Fig. 4:** Measurement result of a pedestrian passing a car, using a effective frequency deviation of 0.5 GHz (a) no AR-LP (b) with AR-LP, and 1.35 GHz (c) no AR-LP (d) with AR-LP at a center frequency of approx. 78 GHz (AR-LP is applied to velocity domain).

further to 1.35 GHz improves the separation of the merged peaks in the range domain, affecting the separation as well in the velocity domain (see Fig. 4 (c)). Thus, applying higher frequency deviation reduces the superposition of the scattering centers of the car and the nearby passing pedestrian without using additional signal processing. However, combining AR-LP for velocity processing and increasing the frequency deviation improves the separation of the moving pedestrian and the car, illustrated in Fig. 4 (d).

## 4 Micro-Doppler signature of slow moving targets

Human motion involves the periodic movement of different body parts such as head, torso, two arms and two legs. High separation abilities in the velocity domain allow the extraction of these contributing elements of an object, called micro-Doppler signature (μD-signature). Additional target information can be extracted apart from the geometric extension of the object and the mean velocity [9] and can be fed to successive Kalman tracking to improve object classification [10], [11].

It has been observed that the periodic movement of torso and legs are the main contributions to the µD-signature. Within the walking cycle, the torso is moving with a nearly constant mean velocity. However, the legs de- and accelerate depending on the actual stance or swing phase [12]. The stance phase is defined as the moment when the foot is on the ground, and the swing phase when the foot is off the ground. The feet alternate roles in a periodic manner as each foot in turn accelerates and reaches a maximum velocity followed by deceleration to zero velocity. Measurement results have shown that the maximum velocity of the pedestrian can be up to three times that of the mean walking velocity due to the acceleration sequence of the leg in the swing phase.

## 4.1 Comparison of pedestrian and car signature

To compare the range-Doppler profile of a moving pedestrian and a car, further measurements were done applying measurement setup 1 of Table I without using AR-LP. In Fig. 5 a snapshot of the range-Doppler profile of a longitudinally moving pedestrian (a) and a car (b) is shown. Measurement time was 5.1 ms and an effective frequency deviation was adapted to 0.5 GHz as described in Sec. III-B.

The actual ranges and radial velocities of the departing pedestrian and the car are 10.5 m with a mean radial velocity of 5 km/h and 10 m with a radial velocity of 6.5 km/h, respectively. The car shows no Doppler spread but an extension in the range profile as it moves longitudinally while the Doppler spread of the pedestrian can be seen clearly. In this specific snapshot the pedestrian makes several contributions to the Doppler spectrum. The velocity values of 0 km/h and 10 km/h belong mainly to the legs in the stance and swing phase while the torso has a velocity of 5 km/h. Due to the movement of the pedestrian, this Doppler signature changes between successive chirp sequences. This requires increased velocity resolution to get an exact µD-signature of the pedestrian.

## 4.2 Scheme of processing

To obtain a specific object signature, major contributing µD-elements have to be extracted with a high velocity resolution capability and tracked over several chirp sequences. However, applying AR-LP for each range cell increases the calculation time. To reduce this demand, the velocity resolution improvement can be done adaptively. This requires searching all relevant targets after range compression. Using OS-CFAR allows determining these targets by calculating a dynamic threshold [13]. As the power level of the target exceeds this threshold, all relevant range-cells will be selected. AR-LP is applied only in these selected range cells to improve the velocity resolution. If only a single object is present, the highest power level in the range-Doppler domain is searched again and the corresponding range with its µD-signature is selected, normalized and stored in memory. By tracking a single object, these raw data of successive µD-signatures contribute to the specific object signature.

The following measurements were done with setup 2 of Table I using 31 filter coefficients of the AR-LP and a frequency deviation of 1.5 GHz. The effective frequency deviation was adjusted by post-processing as described in Sec. III-B. Fig. 6 depicts the measurement results of the

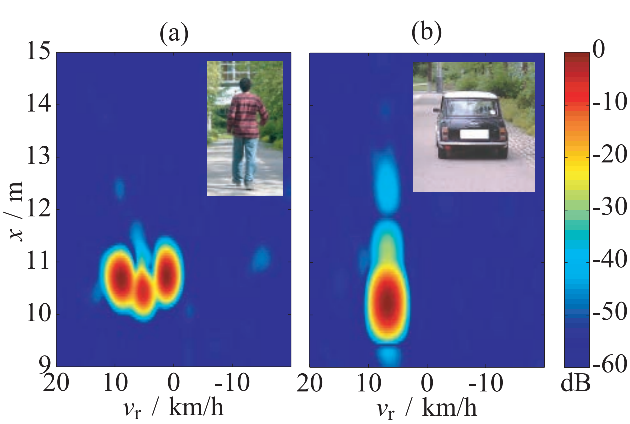


**Fig. 5:** Measurement snapshot of the Doppler profile of a slow moving (a) pedestrian and (b) car ($B = 0.5$ GHz, $f_0 = 78$ GHz) without AR-LP.

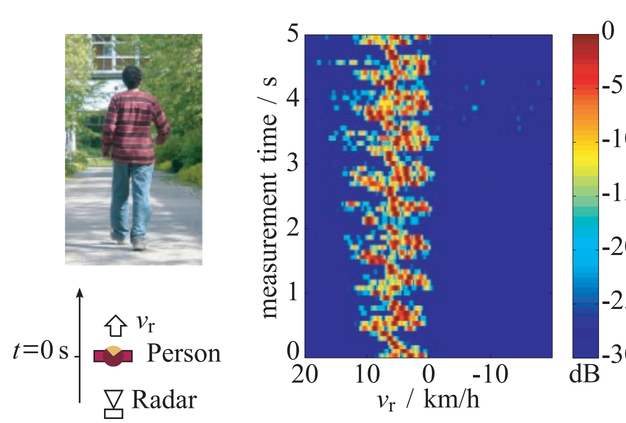


**Fig. 6:** Measurement result of the sequential µD-signature of a pedestrian ($B = 0.5$ GHz, $f_0 = 78$ GHz) using adaptive AR-LP for velocity processing.

sequential µD-signature using an effective frequency deviation of 0.5 GHz at a starting frequency of 78 GHz. At t = 0 s the pedestrian reached the distance of 10 m and was departing with a constant velocity during the measurement time of 5 s. At the distance of 15.8 m the mean velocity was 4.2 km/h. The sequential µD-signature results in a periodic repetition from the movement of the pedestrian. The legs in the stance phase produce a minimum velocity of 0 km/h and in the swing phase a maximum velocity of approximately 10 km/h. The torso meanwhile has a mean velocity of approximately 4.2 km/h. Observing two successive stance and swing phases within a time duration of approximately 1.2 s, allows the walking cycle and hence the step size of 1.4 m to be estimated.

### 4.3 Influence of the frequency deviation

To compare the influence of the frequency deviation on the sequential µD-signature of a departing pedestrian, the recorded measurement data of the previous measurement are processed again with an effective frequency deviation of 1 GHz and 1.5 GHz. In Fig. 7 the measurement results are illustrated. It can be seen that increasing the frequency deviation does not change the Doppler signature of a person significantly, because most contributions of the movement result from the center of the pedestrian. Using a smaller frequency deviation than 0.5 GHz will result in a large range cell size allowing the capture of more contributing µD-elements of the pedestrian. However, separation of the µD-signature in the range-Doppler domain in multi-target scenes, e.g. pedestrian passing a car (see Fig. 4), becomes a more challenging task due to the superposition of all contributing scattering centers.

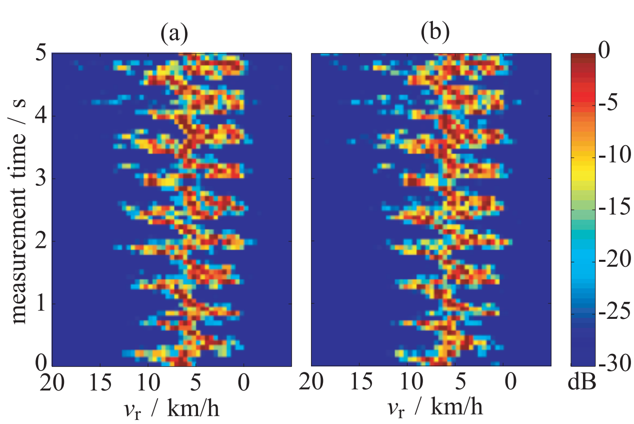


**Fig. 7:** Measurement results of the frequency deviation influence on the sequential µD-signature of a pedestrian at (a) 1 GHz, (b) 1.5 GHz using adaptive AR-LP for velocity processing.

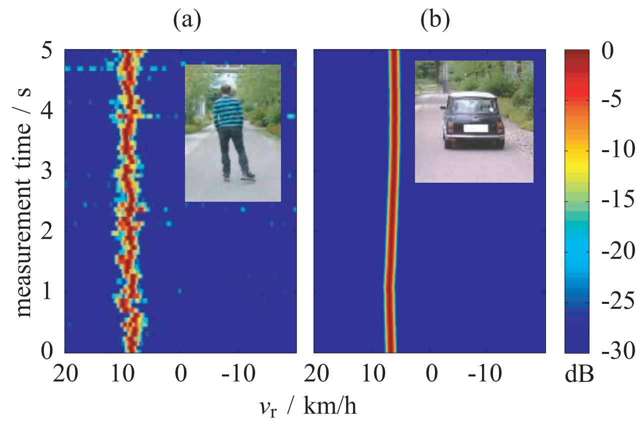


**Fig. 8:** Comparison on the sequential µD-signature of a (a) car and (b) inline-skater using adaptive AR-LP for to velocity processing ($B$ = 0.5 GHz, $f_0$ = 78 GHz).

### 4.4 Influence of the target type

In a multi-target environment radar sensors have to cope with different target types, hence further investigations have been made to see if a car or an inline-skater can be distinguished from a person. The movement of an inline-skater differs from a pedestrian. While the inline skater is in motion with a higher constant velocity than the pedestrian walking speed, the inline skater does not provoke a stance but rather a sliding phase. As a result, no contributing µD-element at 0 km/h will appear. In Fig. 8 (a) the inline-skater shows a remarkably smooth µD-spread compared to the moving pedestrian of Fig. 6. Moreover, it can be seen in Fig. 8 (b) that the strongest scattering center of the car has no µD-spread as it departs, which allows distinguishing between these objects.

## 5 Conclusion

Signal post-processing techniques, like the auto-regressive linear prediction, enables FMCW radar sensors with chirp sequence modulation to improve velocity resolution significantly. Hence, slow-moving targets like pedestrians can be identified at an early stage to avoid or mitigate an accident. The proposed chirp-sequence processing model can be applied to analyze the effect of varying radar system parameters, and can evaluate real radar sensor systems. Furthermore, it is shown that the separation of a vehicle and a nearby pedestrian can be improved by enhancing the velocity resolution with signal post-processing in combination with increased frequency deviation. Finally, AR-LP can be applied to the sequential µD-signature of a car, pedestrian, and inline-skater to distinguish the object type by adaptively increasing the velocity resolution.

## Acknowledgement

This work is funded by the German Federal Ministry of Education and Research (BMBF) under the joint project Radar on Chip for Cars (RoCC).

Received: July 25, 2012.

## References

[1] R. L. Knoblauch, M. Pietrucha, and M. Nitzburg, "Field studies of pedestrian walking speed and start-up time," *Transportation Research Record 1538*, pp. 27–38, 1996.

[2] V. Chen, "Analysis of radar micro-doppler with time-frequency transform," in *Statistical Signal and Array Processing, 2000. Proceedings of the Tenth IEEE Workshop on*, 2000, pp. 463–466.

[3] V. Winkler, "Range doppler detection for automotive FMCW radars," *Proc. European Radar Conference EuRAD 2007*, pp. 166–169, 2007.

[4] M. Andres, W. Menzel, H.-L. Bloecher, and J. Dickmann, "Detection of slow moving targets using automotive radar sensors," in *Microwave Conference (GeMiC), 2012 The 7th German*, March 2012, pp. 1–4.

[5] A. G. Stove, "Linear FMCW radar techniques," *IEE Proceedings F, Radar and Signal Processing*, vol. 139, Issue 5, 1992.

[6] J. Makhoul, "Linear prediction: A tutorial review," *Proceedings of the IEEE*, vol. 63, no. 4, pp. 561–580, April 1975.

[7] S. V. Vaseghi, *Advanced Digital Signal Processing and Noise Reduction*. John Wiley & Sons Ltd, 2000.

[8] P. Feil, W. Menzel, T. P. Nguyen, C. Pichot, and C. Migliaccio, "Foreign objects debris detection (FOD) on airport runways using a broadband 78 GHz sensor," *European Microwave Conference EUMC*, pp. 1608–1611, 2008.

[9] H. Rohling, S. Heuel, and H. Ritter, "Pedestrian detection procedure integrated into an 24 GHz automotive radar," pp. 1229–1232, May 2010.

[10] F. Foelster, H. Rohling, and H. Ritter, "Observation of a walking pedestrian with a 24 GHz automotive radar sensor," *GeMic Karlsruhe*, March 2006.

[11] S. Heuel and H. Rohling, "Two-stage pedestrian classification in automotive radar systems," pp. 477–484, Sept. 2011.

[12] J. Perry, *Gait analysis: normal and pathological function*. Thorofare, NJ: Slack, 1992.

[13] H. Rohling, "Radar CFAR thresholding in clutter and multiple target situations," *Aerospace and Electronic Systems, IEEE Transactions on*, vol. AES-19, no. 4, pp. 608–621, July 1983.